

UC San Diego

UC San Diego Electronic Theses and Dissertations

Title

Identifying suppressors of basement membrane mutants: srp-1 suppresses spon-1 variably abnormal and lethal phenotypes

Permalink

<https://escholarship.org/uc/item/0m87p6ff>

Author

Ho, Tiffany

Publication Date

2018

Peer reviewed|Thesis/dissertation

UNIVERSITY OF CALIFORNIA, SAN DIEGO

Identifying suppressors of basement membrane mutants: *srap-1* suppresses
spon-1 variably abnormal and lethal phenotypes

A thesis submitted in partial satisfaction of the
requirements for the degree Master of Science

in

Biology

by

Tiffany Wing Yin Ho

Committee in Charge:

Andrew Chisholm, Chair
Yishi Jin
Stanley Lo

2018

Copyright
Tiffany Wing Yin Ho, 2018
All rights reserved.

The thesis of Tiffany Wing Yin Ho is approved, and it is acceptable
in quality and form for publication on microfilm and electronically:

Chair

University of California, San Diego

2018

DEDICATION

I would like to thank Professor Andrew Chisholm and all the members of the Jin and Chisholm lab for their support and opportunity. I am truly grateful for my mentor, Jennifer Gotenstein, for her help and advice every step along the way.

Thank you to my parents, my brother, and my TC family for their love and support. Their presence and encouragements allow me to go through everyday with a smile.

TABLE OF CONTENTS

Signature Page.....	iii
Dedication.....	iv
Table of Contents	v
List of Tables	vi
List of Figures	vii
Abstract of Thesis.....	viii
Introduction.....	1
Materials & Methods.....	6
Results.....	15
Discussion	21
References	50

LIST OF TABLES

Table 1: Summary of Outcrosses.....	29
Table 2: Final Candidate Genes.....	30
Table 3: Mapping Data.....	31
Table 4: Neuronal and Muscle Marker Transgenes and Strains Used.....	32
Table 5: <i>pxn-2</i> with Neuronal and Muscle Marker Transgenes Generated and/or Imaged.....	33
Table 6: Rescue Strains.....	34
Table 7: Additional Strains Generated for analysis of <i>pxn-2</i> mutants.....	35
Table 8: Primer Sequence.....	36-37
Table 9: Morphology of <i>spn-1</i> Mutants and Rescued Strains.....	38
Table 10: Brood Size of Vab Counts.....	39

LIST OF FIGURES

Figure 1: Predicted Structure of <i>srp-1</i> and Location of Mutants	40
Figure 2: Two point SNP Mapping Strategy to Generate Recombinant Lines.....	41
Figure 3: SNP Sites on Chromosomes.....	42
Figure 4: Final SNP Summary Showing Recombination Occurring Through -0.46 on the Left and +6.80 on the Right	43
Figure 5: Genetic Cross of Transgenic Fosmid Animals with <i>ju430:ju1185</i>	44
Figure 6: Lethality and Abnormality of Mutants and Rescued Lines	45
Figure 7: Genetic Crosses and Fluorescent Marker Strain Generation.....	46
Figure 8: Imaging of Suppressed and Unsuppressed <i>pxn-2</i> using GABAergic Marker	47
Figure 9: Imaging of Suppressed and Unsuppressed <i>pxn-2</i> using Cholinergic Marker	48
Figure 10: Imaging of Suppressed <i>pxn-2</i> using Synaptic & Whole Neuron Cholinergic Markers.....	49

ABSTRACT OF THE THESIS

Identifying suppressors of basement membrane mutants: *srap-1* suppresses *spon-1* variably abnormal and lethal phenotypes

by

Tiffany Wing Yin Ho

Master of Science in Biology

University of California, San Diego, 2018

Professor Andrew Chisholm, Chair

Spon-1 and *pxn-2* are essential basement membrane genes crucial to the elongation stage of *C. elegans* morphogenesis. However, the interactions of these proteins with other components of the basement membrane and the extracellular matrix are not very well known. In attempts to find factors that interact with *spon-1* and *pxn-2*, EMS screens of both mutants were performed. A suppressor of *spon-1* mutants, *ju1185*,

was isolated from the *spon-1* screen. We mapped this suppressor to chromosome II between -0.46 and +6.80 using two-point mapping with SNPs. Our rescue experiments suggests that this is a missense mutation in *srap-1*. We found that overexpression of this gene also suppresses *spon-1* suggesting that this may be a gain-of-function mutation. In the *pxn-2* mutant screen, a previously isolated suppressor *ju1123* rescued embryonic and larval lethality, but has reduced locomotion due to defects in the synaptic release of acetylcholine. In initial observations of the mutant and suppressor nerve cords of *C. elegans*, we observed an abnormal separation of the dorsal nerve cord axon bundle and GABAergic synapses in commissures. With these observations, we hope to find the relationship between the separations of the nerve cord to *pxn-2*'s role in synaptic vesicle release. These results can potentially reveal additional roles played by these basement membrane genes, as well as discover additional genes essential in morphogenesis, applicable to the study of the epithelia in vertebrates.

Introduction

The epithelial layer is one of four major types of tissues in animals, including muscle, connective, and nervous tissue. It encompasses the epidermis and the surfaces of various organs and glands in the digestive, reproductive, and secretory systems (Ganz, 2002). Epithelial tissues are the first line of defense for the host organism against environmental bacteria and send signals to begin the inflammatory response during barrier breakages (Ganz, 2002). It is also important in absorption and secretion of nutrients and enzymes for respective systems.

Caenorhabditis elegans, a nematode worm, serves as an excellent genetic model for understanding the epithelial tissue development process and interactions of nervous system genes because of its completely sequenced genome, rapid life cycle, and transparency (Corsi et al., 2015). The epidermis is the worms' largest organ and forms the shape and size of the worm allowing for morphogenesis (Chin-sang and Chisholm, 2000). The apical side of the *C. elegans* epidermis secretes a collagenous cuticle layer, while the internal basal side is covered by a basal lamina or basement membrane (Chisholm and Hsiao, 2012). This basement membrane is a specialized type of extracellular matrix that supports the epidermis and provides mechanical stability between the epidermis and muscle tissues (Kramer, 2005). Mutations in basement membrane genes have been shown to be detrimental to the morphogenesis process (Morrissey and Sherwood, 2015).

In order to understand the different basement membrane mutations, it is important to understand the process by which *C. elegans* develops from an embryo to

an adult animal. The *C. elegans* embryonic morphogenesis process includes gastrulation, closure of ventral cleft, dorsal epidermal intercalation, ventral epidermal closure, and elongation (Chin-sang and Chisholm, 2000). Gastrulation begins with an ingression on the ventral side of the embryo due to the movement of intestinal, germline, and mesoderm precursor cells (Chin-sang and Chisholm, 2000). To close this ingression, ectoderm cells will then move together to seal the ventral cleft, as it is called (Chin-sang and Chisholm, 2000). At this point, epidermal cells will have differentiated, which allows the two rows of dorsal epidermal cells to intercalate into the dorsal epidermis (Chin-sang and Chisholm, 2000). On the ventral side, the epidermis will enclose the embryo (Chin-sang and Chisholm, 2000). Finally, during the elongation stage the embryo elongates to about four times its original length due to actin contraction forces in the circumference of the worm embryo (Chisholm and Hardin, 2005). The elongation stage is also broken up into the comma stage, where the worm is in the shape of a comma, as well as the 1.5-fold, 2-fold, 3-fold stage to describe its length compared to the embryo (Chisholm and Hardin, 2005).

SPON-1, a protein of the spondin family, has been found to be essential in *C. elegans* embryonic morphogenesis, especially in the elongation stage (Woo et al., 2008). Spondins are conserved in vertebrates and were originally found to be important in axon guidance (Klar et al., 1992). A study by Woo et al. discovered that *spn-1* is essential in epidermal elongation and muscle attachment with mutants displaying phenotypic defects such as, dumpy, variably abnormal (Vab), or even fully penetrant embryonic and larval lethality (2008). The *spn-1(ju430ts)* allele was found in a screen

for mutations that cause arrest in late stage elongation and muscle detachments; this allele is temperature sensitive and is not viable at 25°C (Woo et al., 2008). It was mapped to the *spon-1* gene as a missense mutation in the fourth thrombospondin type I repeat (TSR 4) (Woo et al., 2008).

In order to identify genes that interact with *spon-1*, an ethyl methanesulfonate (EMS) screen was performed on *spon-1* mutants. EMS is a chemical mutagen that induces mutations in the germline (Kutscher and Shaham, 2014). This method allowed for exploration of other essential genes that are important for the elongation process. EMS treated worms were tested at 25°C and viable worms were isolated as suppressors. *ju1185* was isolated as one of these *spon-1* suppressors; however not much is known about this suppressor at this point, so this study will explore the location, function, and interaction of this suppressor with other components of the epidermal cytoskeleton.

One method to identify a gene is to perform a two-point mapping screen with single nucleotide polymorphisms (SNPs). SNPs are genetic variations that can be used as genetic markers to measure recombination between chromosomes (Fay, 2008). SNP mapping will be done in two phases. The first phase is chromosome mapping in which the relevant chromosome and relative position of the gene is identified. The second phase is interval mapping where the gene is found in an interval between two SNPs. Using this method to generate a set of mapping data along with whole genome sequencing, we can narrow down the genes involved in suppression. This research will contribute to the efforts to decipher the process of *C. elegans* morphogenesis. It can

give insight into the proteins that make up the basement membrane, as well as the epithelial layer on the whole, essential to the elongation process.

Another essential basement membrane gene is PXN-2, a peroxidase protein crucial to late stage elongation (Gotenstein et al., 2010). Loss of this gene causes detachment between muscle and epidermis, thus disrupting the elongation process (Gotenstein et al., 2010). In *pxn-2* mutants, defects such as variably abnormal epidermal morphology (Vab phenotype), body muscle and epidermis tissue detachment, as well as embryonic and larval arrest were observed (Gotenstein et al., 2010). Embryonic arrest or un-hatched eggs are seen in stronger or more lethal *pxn-2* mutant alleles, such as *tm3464*, which never produces viable adult animals. Weaker or less lethal *pxn-2* mutant alleles are characterized by partial larval and embryonic lethality and the Vab phenotype.

A different EMS screen was performed for *pxn-2* mutants conducted in the same manner as the *spn-1* EMS screen, but isolating for worms that do not show the Vab phenotype. One of these suppressors, *ju1123*, was previously mapped to the *let-805* gene (Gotenstein, unpublished data). This suppressor was observed to only rescue the larval lethal phenotype found in *pxn-2* mutants, but not the locomotion defect phenotype (Gotenstein, unpublished data). In order to explain this partially rescuing phenotype, aldicarb, an acetylcholinesterase inhibitor that causes a buildup of acetylcholine (ACh) in the synapses and hypercontracted paralysis in the worms (Rand, 2007), was used to observe the response of *pxn-2* mutants. Results of this assay showed that *pxn-2* mutants are resistant to aldicarb (Fukuda, unpublished data). This indicated that there

was abnormal functioning of synapses in *pxn-2* mutants due to either the release of ACh or the uptake of ACh by the muscle receptors. To pinpoint the cause of the problem levamisole, a nicotinic acetylcholine receptor agonist that also causes hypercontracted paralysis in the worms, was used (Rand, 2007). The results of the assay showed that *pxn-2* mutants are sensitive to levamisole (Fukuda, unpublished data), thereby rejecting the possibility that there are problems with the muscle receptor and suggesting that there are defects in the release of acetylcholine from synapses. Given these observations, this study will further seek to understand neuronal and muscle synaptic morphology in suppressed and unsuppressed *pxn-2* mutants that can potentially explain its partially rescuing phenotype. In the greater scope, this research can contribute to revealing additional roles that *pxn-2* play in the basement membrane and the extracellular matrix.

Materials & Methods

Two-point mapping screen with single nucleotide polymorphisms

In SNP mapping, the first step is to cross wildtype N2 males with the mutant strain to create heterozygous progeny (Figure 2). The F1 progeny are allowed to self-reproduce and homozygous F2 progeny are isolated as mapping lines to detect whether recombination occurred. If the gene of interest is located on the same chromosome as the SNP tested, an over representation of the mutant strain is expected in the mapping lines. On the other hand, if the gene of interest is on a different chromosome than the tested SNP, the mapping lines will segregate in a 1:2:1 ratio of mutants, heterozygotes, and wildtype, as in typical Mendelian ratio. To further narrow down the region in interval mapping, recombination is observed across adjacent SNP sites within a single mapping line. Since recombination occurs by chance during meiosis, it is necessary to generate many mapping lines to observe the extent of recombination between wildtype and mutant chromosomes.

Outcrosses of mutants, observation of suppression, and generation of mapping lines

Outcrosses were done by first crossing mutant strains to N2 males. Heterozygous F1s were picked and placed at 15°C. When these plates grew up, Vab F2 worms were singled and placed at 15°C. After 3 days at 15°C, F2 plates were screened for viable worms. From the viable plates, about 10 F3 progenies were transferred to new plates and placed at 25°C. This was done over 2-3 days because some plates grew up

slower than others. After 5 days at 25°C, each F3 plate was screened for viable progeny and assigned a score of suppression level.

Viable progeny was rated on a scale of 1-5: 1 signified no progeny or no suppression, 3 represented moderate suppression or unsure, and 5 stood for lots of progeny or homozygous suppressor. For F3 plates that had fewer worms to begin with, the rating was scaled up to adjust for the differences. The amount of unhatched eggs was also observed on a scale of 1-5, with 1 meaning no unhatched eggs, 3 meaning some unhatched eggs, and 5 representing lots of unhatched eggs.

The generation of mapping lines was done using essentially the same protocol, except only single F3 worm were transferred to new plates and placed at 25°C. The F3 plates were screened for viability after 3 days. These viable plates became mapping lines and were designated a number for tracking during the mapping process.

Designing primers and digestion sites

The whole genome sequencing results of *ju1185:ju430* (CZ20595) were run through the Mercury program (McCulloch et al, 2017). A SNP site was chosen by filtering through the range of interest. Then, the reference sequence of the chosen SNP site was BLASTed on Wormbase to make sure there are only one or few matches. Next, we checked that there were available enzymes in the “Site Lost” column to ensure that N2 bands are cuts and mutant bands do not. The reference base number was used to retrieve the sequence in Mercury. This sequence was then copied to the ApE program and the enzyme cut sites were checked first. Once we made sure that there was only

one cut site at the SNP change and within 100bp from the SNP, we can confirm that the enzyme can be used for digestion.

The primers were designed at least 100bp away from the SNP site and BLASTed on Wormbase to check that they are unique. The forward primers were designed in the 5' to 3' direction and the reverse primers were designed in the 3' to 5' direction. To produce better PCR product, the melting temperatures of the forward and reverse primers were designed similarly. Finally, we checked that the N2 bands after digestion were different lengths, in order to be able to distinguish them on a gel.

Genotyping SNP sites

The worm lysis for the mapping lines and controls were made by submerging a clump of worms in 50 μ l of lysis buffer and setting it in 65°C for 1 hour and 95°C for 15 minutes. Primers were tested using N2 and CZ20595 for the correct size bands after digestion. After primers were confirmed to be working, PCR reactions were setup for all of the mapping lines. The PCR reactions included homemade 10x PCR buffer, dNTP, MgCl₂, Taq polymerase, forward/reverse primers, ddH₂O, and DNA lysis. The PCR program used was a Touchdown program, which decreased by 0.5°C from 62°C to 54°C during the annealing step every cycle for the first 16 cycles, then remained at 58°C during the annealing step for the last 16 cycles. Next, the PCR product was digested using the designated enzyme for the specific primer set (Table 8). Each digestion reaction was setup using 2 μ l cutsmart buffer, 0.3 μ l enzyme, 7.7 μ l ddH₂O, and 10 μ l PCR

product. The digestion was incubated at 37°C for 3 hours. This was visualized on a 1-2% agarose gel depending on the expected band sizes.

Fosmid prep

The protocol for fosmid prep was adapted from Epicentre. First, the fosmid (WRM0626cC02) was grown overnight in 100ml of LB, 25 μ l of 50 mg/ml chloramphenicol, and 16.6 μ l of 75 mg/ml ampicillin. The bacteria culture was pellet at 4K rpm for 20 min and resuspended in 3ml of P1. To lyse the cells, 3ml of P2 was added and inverted gently. Then, 3ml of cold P3 was added, inverted, and left on ice for 5 mins. The mixture was centrifuged for 10 minutes at 4K rpm and the supernatant was transferred to a polypropylene tube. This was spun for 15 minutes at 14K in 4°C. The clear supernatant is transferred to a new tube and 4.5ml of isopropanol was added. This mixture was incubated at -20°C for 30 minutes and then centrifuged again for 15 minutes at 14k in 4°C. The supernatant was discarded and the pellet was let dry for 5 minutes. Then, it was resuspended in 500 μ l of TE buffer and transferred to a microcentrifuge tube. Next, an RNase treatment was done by adding 1 μ l of 10mg/ml RNase A and incubated in a 37°C water bath for 25 minutes. After, 500 μ l of 5M ammonium acetate was added, inverted, and incubated on ice for 15 minutes. This was centrifuged in a 4°C tabletop centrifuge for 10 minutes and maximum speed. The supernatant was transferred to a clean microcentrifuge tube and 0.6 ml of isopropanol was added. This was incubated at -20°C for 20 minutes, then centrifuged for 10 minutes in a tabletop centrifuge. The supernatant was removed and 150 μ l of 70% ethanol was used to wash the pellet. Finally, this was centrifuged at 14K for 10 minutes and the

supernatant was removed. The pellet was air-dried for 10 minutes and resuspended in 100 μ l of EB buffer.

Fluorescent marker prep

The fluorescent marker Pmyo-2-mcherry was miniprepmed using the Purelink HiPure Plasmid Miniprep kit. An overnight culture was set up with ampicillin as the antibiotic resistance marker. First, the mini columns were equilibrated with 2ml of equilibration buffer and allowed to drain by gravity flow. Then, the overnight cultures were transferred to microcentrifuge tubes and centrifuged at 14,000 rpm for 3 minutes. The medium was removed and the pellet was resuspended in 0.4ml of resuspension buffer. The homogenous mixture was lysed by adding 0.4ml of lysis buffer. This was inverted gently five times and incubated for 5 minutes at room temperature. Next, we added 0.4ml of precipitation buffer and mixed immediately by inverting. The lysate was centrifuged at 12,000 rpm for 10 minutes at room temperature. The supernatant was loaded onto the equilibrated column with a pipette and the solution was allowed to drain by gravity flow. We washed the column twice with 2.5ml of wash buffer each time and allowed it to drain by gravity flow again. To elute the purified DNA, we added 0.9ml of elution buffer to the column and allowed it to drain by gravity flow into a sterile microcentrifuge tube. To further wash the DNA, we added 0.63ml of isopropanol to the eluate, inverted, and centrifuged at 12,000 rpm for 30 minutes in 4°C. The supernatant was discarded and 1ml of 70% ethanol was added to the pellet. This was centrifuged again at 12,000 rpm for 5 minutes in 4°C. The supernatant was removed and the pellet was air-dried for 10 minutes before resuspending in 50 μ l of TE buffer.

Injection

The day before injection, we isolated about 40 to 50 L4 stage N2 worms onto a fresh plate. The injection mix for our transgenic fosmid lines was prepared by diluting the fosmid to 20ng/ μ l and the fluorescent marker to 2.5ng/ μ l. In order to have 100ng/ μ l of DNA total, we diluted pBS to 80ng/ μ l. The injection mix for the CRISPR/Cas9 protocol was prepared by diluting our oligo to 500nm, the sgRNA to 50ng/ μ l, and fluorescent marker Pmyo-2-mcherry to 2.5ng/ μ l.

A day 1 adult was transferred to an oil spot on the injection pad. A preloaded injection needle injected the injection mix in the gonads. The worm was quickly recovered by a drop of M9 and transferred to a new seeded plate. The injected worms were placed at 20°C for 3 days and screened for the fluorescent marker. Worms that have the fluorescent marker were picked and the next generation was again screened for the marker.

Rescue suppression by genetic cross of WRM0626cC02 fosmid animals with *ju1185:ju430*

Fosmid injections resulted in three transgenic lines of *srp-1* overexpression (CZ26369-CZ26371). The transgenic fosmid lines were crossed to N2 males (Figure 5). The males expressing Pmyo-2-mcherry were isolated and crossed to *ju430:ju1185* hermaphrodites. From the pool of F1 progeny, the RFP+ hermaphrodites were picked and allowed to self-fertilize. To ensure that the F2 progeny have the fosmid and *ju430:ju1185*, we singled Vab and RFP+ worms. These were allowed to grow at 25°C.

Those that were viable were sequenced for *ju430* with primers AC1642, AC1643. They were not checked for the presence of the *ju1185* mutation because the two mutations are tightly linked. Lines that were homozygous for *ju430* mutation were used in the rescue experiment.

CRISPR/Cas9 deletion mutation design and preparation of sgRNA

The sgRNA sequence was designed using the CRISPR design tool from the Zhang lab at MIT (Zhang, 2017). The sgRNA sequence flanked the region to be deleted and was chosen based on a high specificity score and minimal off-target sequences. The sgRNA sequence was inserted into Peft-3-cas9-NLS-pU6-sgRNA empty vector using mutagenesis primers. The forward primer was designed by 20 basepairs of sgRNA sequences followed by GTTTTAGAGCTAGAAATAGCAAGTTAAAATAAG and the reverse primer was the reverse complement of the 20 basepairs of sgRNA followed by CAAGACATCTCGCAATAGGAG. The vector was amplified by PCR reaction using 32.5 μ l of ddH₂O, 1 μ l of 2.5mM dNTP, 10 μ l of 5x HF buffer, 2.5 μ l of 10 μ M forward and reverse primers, 1 μ l of template plasmid, and 0.5 μ l of Phusion hot start polymerase. The PCR program had annealing temperature of 60°C and elongation for 5 minutes for a total of 35 cycles. The PCR product was ran on a 1.5% gel to yield a 8kb band. After confirmation, the PCR reaction was treated with 1 μ l of DpnI for 1 hour at 37°C to remove the plasmid template. This was transformed into DH5 α competent cells with 5 μ l of PCR reaction. 4 overnight cultures with 1 colony each was setup using 3ml of LB and 4 μ l of 75mg/ml ampicillin. This was mini prepped using the Qiagen miniprep kit and

digested with PshAI at 37°C. Confirmation of correct clones with ~5kb and ~3kb bands were sent for sequencing using YJ10152 pU6-F primer. After confirmation of the correct sgRNA sequences, the colonies were mini prepped using the Invitrogen Purelink HiPure Plasmid Miniprep kit.

Vab counts

We conducted Vab counts on the two strains made from crossing the transgenic fosmid lines with our suppressor *ju430:ju1185* (CZ26372-CZ26373). As controls, we did Vab counts on the unsuppressed mutant *ju430* and suppressed mutants *ju430:ju1185* (CZ20595). The experiment was performed at 25°C.

On day 1, five L4 staged worms from each strain were singled. These parent worms were transferred to new plates on day 2. On day 3, we looked back at the day 1 plates and counted the embryos on the plates, differentiating between the RFP+ and non-RFP embryos. The parent worms on day 2 plates were also transferred to new plates. On day 4, the larvae on day 1 plates and the embryos on day 2 plates were counted, differentiating between RFP+ and non-RFP embryos and worms. The parent worms on day 3 plates were transferred to new plates. On day 5, the adult worms on day 1 plates were counted, differentiating between Vab, non-Vab, RFP+, and non-RFP worms. The larvae on day 2 plates and the embryos on day 3 plates were also counted. The parent worms on day 4 plates were removed. On days 6, 7, 8, the adult worms were counted from the day 2, 3, 4 plates, respectively, again differentiating between Vab, non-Vab, RFP+, and non-RFP worms.

Genetic crosses and fluorescent marker strain generation

Strains were maintained on NGM agar plates at 20°C. N2 males were crossed to hermaphrodites with the fluorescent marker (Figure 7). The heterozygous F1 males were picked and crossed to a *pxn-2* mutant or the suppressor of *pxn-2* mutant. Heterozygous F2 progenies were singled and allowed to grow up at 20°C. These plates were screened for Vab and fluorescent worms. Finally, the fluorescent marker was homozygoused by screening for all fluorescent progenies. The mutant allele *ju358* was homozygoused by sequencing. The mutant allele *tm3464* was homozygoused by PCR with primers AC1752, AC1744, AC2047. The suppressor allele *ju1123* were homozygoused by PCR with primers AC3299, AC3300 and digested with MsiI.

Imaging of synaptic and neuronal phenotype

Worms were imaged on the LSM-710 confocal microscope. Slides were generally prepared with an agarose pad and a drop of M9 solution. Different worm immobilization protocols were used. This included a 10% agarose pad with 0.2 μ l of M9, 10% agarose pad with 1-Phenoxy-2-propanol (POP) in M9, or a 10% agarose pad with beads. An adult worm was picked and placed on the slide and transferred to the microscope to image. The dorsal and ventral sides of the same worm were imaged in the same region.

Results

Chromosome mapping

To map a single gene out of the entire genome, it is useful to first narrow down to a single chromosome. We turned to our whole genome sequencing results to decide which chromosome has the most likely candidates. On chromosomes I, III, IV, V, and X, we saw a list of about 20-30 SNPs with common SNPs subtracted. On chromosome II there were over 60 SNPs detected, even with common SNPs subtracted. We chose SNP sites near the ends and middle of each chromosome to test for recombination.

Using outcrossed mapping lines 1 to 34, Chromosome V showed a roughly even frequency of mutant (S) and wildtype (N2) genotypes at positions -17.81 and -11.7. SNP position -17.81 showed a 67% frequency of wildtype genotypes and 33% mutant genotypes, while position -11.7 showed 55% wildtype genotypes and 45% mutant genotypes (Table 3). The even spread of mutant and wildtype genotypes was also observed in chromosome I at -2.89 and +2 sites, as well as chromosome II +22.96. In contrast, there is an overrepresentation of mutant frequencies at I+28.42, II-15.59, and II+3.36. Chromosome I+28.42 showed 92% mutant frequency, chromosome II-15.59 showed 74% mutant frequency, and chromosome II+3.36 showed 94% mutant frequency (Table 3).

Outcross of suppressor showed linkage to *ju430* on chromosome II

The suppressor was outcrossed to N2 males. There were 29 plates of F3 progeny placed at 25°C. The average rating for all 29 F3 plates was 4, meaning more viable progeny than moderate suppression, but less than homozygous suppression. The

lower ratings were mostly given to slower growing F3 plates and plates with less F3 worms to begin with. To summarize, *ju430;ju1185* showed 72.4% suppression (Table 1).

Additional outcrosses with known linked and unlinked suppressor mutant genes were performed. *ju430;ju1198* served as unlinked suppressor mutant genes. From this outcross, 28 plates of F3 progeny were placed at 25°C. There was a 53.6% suppression observed from these worms (Table 1). *ju430;ju1191* served as linked suppressor mutant genes. There were 12 plates of F3 progeny tested at 25°C. We observed a suppression level of 83.3%. *ju430* mutant served as a negative control with 0% suppression when placed at 25°C.

Initial two point SNP mapping narrowed down region between II -6.31 and +0.94

With the conclusion that suppressor *ju1185* is linked to *ju430* on chromosome II, we focused on narrowing down the region on chromosome II. Starting with the right arm of chromosome II, we designed primers for SNP sites: +0.94, +3.13, +3.36, +3.79, +6.80, +12.0, +17.03. Using additional mapping lines 1 to 58 from another outcross, we found that recombination occurred through +0.94 for mapping line 8. This allowed us to eliminate the right arm up until +0.94 of chromosome II as the candidate region for our suppressor. Moving to the left arm of chromosome II, we designed primers for SNP sites: -8.26, -6.31. Mapping lines 4, 11, and 58 showed recombination occurring through -6.31. At this point the region of interest is between -6.31 (3.4 Mb) and +0.94 (8.9Mb).

From the whole genome sequencing results, this region included a total of 21 genes. A particular gene of interest was Y8A9A.2, which is a member of a disintegrin and metalloproteinase with thrombospondin-like motifs (ADAMTS) family.

Final two point SNP mapping narrowed down region between II -0.46 and +6.80

A new batch of mapping lines were made by another round of outcrossing, resulting in a total of 90 mapping lines made in total. Further mapping was done on the left arm of chromosome II using SNP sites -4.74, -2.54, -1.07, -0.98, -0.46. Genotyping the new mapping lines using these SNP sites showed recombination occurring through -0.46. On the right arm, we found recombination through +0.76 using mapping line 8. This allowed us to narrow the region of interest between -0.46 (6.1Mb) and +0.76 (8.3Mb) and further eliminate the list of candidate genes down to 10 genes.

In order to check this region, we genotyped SNP sites +3.13, +3.36, +3.79, +6.80, +12 using the new batch of mapping lines. We found that recombination only occurred through +6.80. With this new mapping data, we decided the final region of the suppressor is between -0.46 and +6.80 (Figure 4). Within this region, the whole genome sequencing results showed that there were ten different candidate genes subtracting genes that were commonly found in the *ju430* background (Table 2). One of these candidates was *srap-1*, which we chose to test for rescue.

Overexpression of *srap-1* partially abrogates suppression of *ju1185: ju430*

We generated two correct transgenic fosmid lines with the suppressor in the background (CZ26372, CZ26373) verified by sequencing for *ju430* and checking for RFP+ worms under the dissecting microscope (Table 6). These worms were placed at 25°C as well as 15°C. For controls, *ju430:ju1185* (CZ20595), *pmyo-2:juEx7869*, and *pmyo-2:juEx7871* (CZ26369, CZ26371) strains were also placed at 25°C and 15°C. After 3 days at 25°C, we found that the transgenic suppressor strains (CZ26372, CZ26373) did not suppress. The control transgenic lines were growing as expected. However, the control suppressor strain was growing slowly at 25°C.

A further experiment was done to test the control suppressor strain at 25°C along with the transgenic suppressor strains. Again, after 3 days at 25°C, we found that the transgenic suppressors rescued the suppression. Re-testing of the control suppressor at 25°C showed suppression as expected. This preliminary experiment showed some rescue of suppression to lethality with a fosmid transgene.

Increased in suppression found in *srap-1* overexpression lines

In the transgenic suppressor strains, we found a significant increase in suppression compared to the suppressor alone. Embryonic lethality in transgenic worms was suppressed by 3-fold compared to the original *ju430:ju1185* worms (Figure 6). Adult Vab worms dramatically increased from about 3% to 60% of the total transgenic worms.

Furthermore, lethality is significantly higher in non-transgenic worms compared to transgenic worms within the transgenic suppressor strains. Adult Vab worms increased from about 10% to 60% from non-transgenic to transgenic worms.

The total brood size of the transgenic suppressor strains (average 86.8) is comparable to the suppressor alone (average 104.25) (Table 10). The average brood size of the transgenic suppressor was calculated with 2 strains of 5 worms each, while the average brood size of the suppressor alone was calculated with 4 worms because a parent worm crawled off the plate on day 4 of Vab counts. Finally, the transgene is transmitted to 13% of progeny at 25°C, as an average between the two transgenic suppressor strains.

In our *ju430* mutant, we did not see 100% lethality at 25°C, as expected, instead our Vab count showed 61.3% mean lethality (Figure 6). This may be the result of a spontaneous mutation that arose over time. This has precedent in *pxn-2 (ju358)*, where the suppressor *vab-10 (ju958)* appeared spontaneously.

CRISPR deletion to create *ju1185* missense mutation in *ju430* background

We injected 20 *ju430* worms with the pre-designed oligo and sgRNA injection mix. These worms were placed at 15°C to grow. After 6 days at this permissive temperature, five parent plates were found to express the Pmyo-2-mcherry coinjection marker. From these five parent plates, 30 F1's were singled and grew at 15°C for 3 days. After these worms grew to L4 stage, we shifted them up to 25°C to observe for suppression. After 3 days, many Vab and non-viable L1 staged worms were found on

the plates, although some showed signs of viable progeny. These potential plates were sent for sequencing with *srap-1* primers (AC4095, AC4096). However, the sequencing did not confirm the intended nucleotide changes in the worms.

Synaptic and neuronal morphology in suppressed and unsuppressed *pxn-2*

Observations on synapses and neurons were made using cholinergic markers *nuls94* and GABAergic marker *juls1*. The synaptic morphology was consistent between the suppressed and unsuppressed *pxn-2* mutants in both cholinergic and GABAergic synapses. However, the cholinergic marker showed an abnormal separation of cell bodies and synapses in mutant and suppressed strains, especially found in the ventral cord (Figure 9). The GABAergic marker showed synapses in the commissures of the mutant's ventral cord (Figure 8). Overall, both the ventral and dorsal cords appeared wavier than wildtype.

To further look at the neuronal and synaptic phenotypes, we made the strain *nuls321; nuls152; ju1123; tm3463* to observe the cholinergic neurons and synapses in a single animal. We saw a slight separation of the dorsal cord axon bundle from imaging, which was not seen in wildtype (Figure 10).

Discussion

Mapping of *ju1185* suppressor

The whole genome sequencing results initially left us with an overwhelming list of hundreds of candidate genes for our suppressor. We were able to eliminate all of the chromosomes except chromosome II through initial chromosome mapping. Further mapping and rescue experiments allowed us to settle on a set of 10 final candidates for our suppressor.

In the initial chromosome mapping, the plus end of chromosome I as well as chromosome II were areas of interest because high rates of recombination events were observed. An overrepresentation of the mutant genotype is expected if the gene of interest is located on the same chromosome as the SNP tested. This is because when they are in close proximity, there is a lower chance that recombination will occur between the mutant and SNP, but a higher chance that the mutant and SNP will recombine together. The high rates of recombination observed at the plus end of chromosome I, also the plus and minus ends of chromosome II did not allow us to narrow down to one chromosome. Thus, we turned to a different method to narrow down to a single chromosome.

Given the difficulty to separate our suppressor and *ju430* during outcrosses, we held some suspicions that they are closely linked together on chromosome II. We outcrossed the suppressor strain along with several other known linked and unlinked strains to *ju430*. Our expectation was that linked genes would produce a higher percentage of suppression because there is lower chance that the suppressor gene and

mutant gene would separate from recombination. Unlinked genes would show a comparably lower percentage of suppression because there is a higher chance that these genes would separate during recombination. We found this to be true with linked genes *ju430; ju1191* having a relatively high level of suppression (83.3%) and unlinked genes *ju430; ju1198* having a comparably lower suppression (53.6%). Our suppressor showed a 72.4% level of suppression similar to the linked control, allowing us to conclude that our suppressor is linked to *ju430* on chromosome II and eliminating chromosome I from our focus.

In mapping of chromosome II, we used mapping lines that we generated through multiple rounds of outcrossing. The mapping lines were used to detect recombination along chromosome II at specific sites that we tested through SNPs. Each recombination event detected allowed us to narrow down the region in which our suppressor is located. The initial two point SNP mapping narrowed the region down to -6.31 and +0.94 on chromosome II. Within this region, 21 genes were included from the WGS results. From this candidate list, *Y8A9A.2* was particularly of interest because this gene is part of the disintegrin and metalloproteinase with thrombospondin-like motifs family. Since *spn-1* has multiple known thrombospondin-like motifs and *ju430* has a missense mutation in the fourth thrombospondin type I repeat, it is possible that a suppressor of *spn-1* lethality contains the same motifs. Furthermore, other proteins of this family, including MIG-7 and GON-1, localize to the gonad basement membrane and interact with collagen IV (Kim, 2015). SPON-1 is also expressed in the basement membrane and interacts with collagen IV. Therefore, it is likely for our suppressor to be expressed in the

basement membrane to suppress *spn-1* mutant lethality. These qualities made Y8A9A.2 an attractive candidate for our suppressor.

In the next round of mapping, we tested SNP sites closer to the middle of chromosome II as well as near *spn-1* at II+0.50. Since our suppressor is closely linked to *spn-1*, we expect that they will be relatively close together on the chromosome. This mapping resulted in II-0.46 and +0.76, including a total of 10 genes. Out of these 10 genes, there were 3 possible candidates for our suppressor. *T14B4.2* is involved in embryo and larval development. It is expressed in the gonad and is part of the small ribosomal subunit. It is a possible candidate because it is involved in development, which is the process our suppressor appears to be affecting. *qua-1* is expressed prior to molting in hypodermal cells. It undergoes cyclical changes during larval development, accumulating prior to molting, and disappearing between molts. It is mostly expressed in the hypodermis. This is a likely candidate because it is involved in the developmental process. *dab-1* is also involved in molting and the developmental process making it a possible candidate. Even though these 3 candidate genes may have possible interactions with *spn-1* according to their known functions, it is difficult to decide which gene is the most likely candidate because these genes have not been found in the same suppressor screen nor are their functions very well known.

Looking back at our mapping data, we noticed that the right arm of chromosome II was eliminated by only mapping line 8. With this line no longer extant, it is difficult to substantiate the mapping of the right arm. Therefore, a new batch of mapping lines was made in another round of outcrossing. The right arm of chromosome II was re-

genotyped with SNP sites that were previously eliminated by mapping line 8. With the new batch of mapping lines, we were able to narrow down to +6.80. This is a wider region than previously thought, but after subtraction of *ju430* background SNPs, we narrowed down to a list of ten different candidate genes. Within the list of ten genes, *srap-1* stood out as a possible candidate of our suppressor because another allele (*ju1179*) from the same EMS screen was previously mapped to this gene (Figure 1).

srap-1, previously named *T06D8.1*, codes for a predicted mucin similar to *Staphylococcus aureus*' serine rich adhesion molecule SraP. The mucin family consists of extracellular matrix proteins secreted by different cell types, including the epithelia (Jones et al, 2013). In a prior study, the researchers hypothesized that a duplication mutation was responsible for the suppression of *rol-3* lethality by either interrupting a gene that leads to lethality or by extra copies of a gene that give rise to suppression (Jones et al., 2012). It was found overexpression of *srap-1* by fosmid injection into *rol-3* (*s1040*) animals that encompassed its entire coding region suppressed *rol-3* lethality (Jones et al., 2012). This was further confirmed by RNAi knockdown of *srap-1* in suppressed animals, which rescued suppression, but dsRNA targeting *srap-1* in wildtype animals did not cause lethality, suggesting that overexpression of *srap-1* is necessary for suppression.

Given that the EMS screen is likely to produce suppressors originating from the same gene and *srap-1*'s history of rescuing lethality, we pursued this gene as our candidate for suppression. We hypothesized that the cytosine to thymine missense mutation in *srap-1* disrupts a gene responsible for lethality in the absence of *spon-1*. We

attempted to use CRISPR/Cas9 to generate the *srap-1* mutation in *ju430* animals. The repair oligo was designed to mimic the *ju1185* missense mutation from cytosine to thymine. The third base pair in the codon was changed as well from GCG to GTC in order to induce a more significant change since the amino acid change is from alanine to valine, which are both nonpolar. This experiment was to no avail, as we could not successfully induce the mutation into a *ju430* background. This could be due to the fact that *ju430* worms are very sick to begin with, thus difficult to revive from injections, although we accounted for this by growing these worms at the permissive temperature of 15°C. We could potentially avoid this problem by instead introducing the wildtype copy of *srap-1* into *ju430;ju1185* worms and rescue the suppression at 25°C. However, this approach may not give us a straightforward answer as we found in the fosmid experiment described next.

Simultaneously, we conducted a rescue experiment similar as described in the 2012 study by Jones et al. Using the same fosmid, we injected the construct into wildtype N2 worms and isolated 3 transgenic lines. These transgenic lines containing our fosmid and co-injection marker *Pmyo-2-mcherry* were crossed to our suppressor strain to create lines that will, in theory, rescue suppression or rescue to lethality at 25°C. However, this experiment may not be conclusive if the suppressor *ju1185* is a dominant mutation because the wildtype copy would not be able to complement. From the rescue experiment, we observed a partial rescue of suppression, which suggests that the fosmid construct reversed the suppression of *ju1185* on *ju430* worms. This may be due to the overexpression of wildtype *srap-1*, which masks the effects of the mutated

ju1185 allele, thus undoing its suppression effects at 25°C. The partial rescue phenotype observed may be due to an unequal amount of wildtype *srap-1* expressed compared to the suppressor allele, which allowed some level of suppression to occur.

To better quantitate the level of suppression that the fosmid construct has on our suppressor *ju1185:ju430*, we performed Vab counts over 8 days. However, instead of an abrogation of suppression by the overexpression of *srap-1*, we found an increased suppression compared to the suppressor alone. Embryonic lethality, which was over 80% in the suppressor alone, decreased, while adult Vabs increased significantly in the transgenic suppressor. These results counter our initial hypothesis that the *ju1185* mutation produces a mutated *srap-1* protein that interrupts a lethal gene, thereby causing suppression. Instead by an alternative pathway, *ju1185* may be a gain-of-function mutation where increased copies of *srap-1* upregulates the machinery that causes suppression. Since *srap-1* is secreted in the extracellular matrix in epithelial cells, as well as many other cell types, it is possible to interact with *spon-1* in the basement membrane. This may not be a direct interaction, as *srap-1* is in the ECM and later secreted in the cuticle during molting, but may involve other intermediate interacting molecules.

Even though our findings do not adhere directly to our hypothesis, we saw an increase in suppression due to the extra copies of *srap-1*. This suggests that *srap-1* is the causative gene for the suppression phenotype we observed in *ju430:ju1185*. By means of an alternative pathway, SRAP-1 may indirectly suppress the lethality caused by basement membrane mutant *spon-1(ju430)*. In order to confidently map the mutation

to *srap-1*, the next step would be to perform genetic crosses of our transgenic *srap-1* array to various other basement membrane mutants, including *spon-1 (ju402)* a null mutation, *pxn-2 (ju358)* a strong mutant, *pxn-2 (tm3464); juEx1044* a null mutation. Suppression of these mutants by an overexpression of *srap-1* would strongly confirm its role in suppression of basement membrane mutants.

Synaptic and neuronal morphology in suppressed and unsuppressed *pxn-2*

The imaging of *pxn-2* suppressed and unsuppressed mutants showed consistent synaptic morphology, but a separation of the cell bodies and synapses found using the cholinergic marker and synapses in the commissures seen using the GABAergic marker. The separations of the cell bodies and synapses can potentially cause a lag in their communication causing defects in the release of acetylcholine from synapses to the muscle receptor. Thereby, hindering the ability to innervate the muscles used in locomotion. The synapses found in the commissures also poses as a problem for the muscle receptors to receive acetylcholine over a long range. The neurotransmitters may be released from the synapses as normal, but the distance they have to travel to the body wall muscles may cause some to be lost.

These variations found in the morphology is the first step in uncovering the differences between a wildtype animal and suppressed *pxn-2* animal, but is not sufficient to explain the partially rescuing phenotype. The next step would be to conduct additional aldicarb and levamisole assays on suppressed *pxn-2* animals. The aldicarb assay would inform us whether there are abnormal functions of synapses in suppressed

pxn-2 animals. This would most likely be true as we saw defective locomotion in these animals. Whereas, the levamisole assays would allow us to see whether the muscle receptors are defective, which would narrow down the causative defect to either acetylcholine release or reception. Furthermore, we can screen for suppressors of this locomotion defect with another EMS screen. The suppressors can reveal to us what other factors are important in fasciculation and thus leading to normal locomotion in *C.elegans*. These results along with the previous morphologic observations would ultimately allow us to pinpoint the reason behind the partially suppressed phenotype observed in suppressed *pxn-2* animals and allow us to learn about the basement membrane's role in the motor circuit

Tables

Table 1: Summary of outcrosses

	Suppressor of interest	Negative control	Positive control (unlinked)	Positive control (linked)
	<i>ju430: ju1185</i>	<i>ju430</i>	<i>ju430; ju1198</i>	<i>ju430: ju1191</i>
No Suppression	4/29 = 13.8%	20/24 = 83.3%	6/28 = 21.4%	0/12 = 0%
Unsure	4/29 = 13.8%	4/24 = 16.7%	7/28 = 25%	2/12 = 16.7%
Suppression	21/29 = 72.4%	0/24 = 0%	15/28 = 53.6%	10/12 = 83.3%

Table 2: Final Candidate Genes

Map Units	Position	SNP	Gene name	Protein/Function/Location	Old AA/new AA
-0.04	6677967	C -> T	<i>H43E16.1</i>	Enriched in intestine, PVD, OLL neurons	A/V
+0.75	8201798	C -> T	<i>qua-1</i>	Expressed prior to molting in hypodermal cells	S/F
+0.76	8323430	C -> T	<i>ran-3</i>	RNAi, embryo development, etc.	G/R
+0.94	8967884	C -> T	<i>szy-20</i>	Negatively regulate centrosomes	G/R
+1.48	9512717	T -> A	<i>gcy-1</i>	Encodes transmembrane guanylyl cyclase	H/L
+2.35	10259741	C -> T	<i>F54B3.1</i>	Embryo development	L/F
+3.13	10797386	C -> T	<i>npp-19</i>	Embryo development, nuclear import, nucleus organization	V/M
+3.36	11218740	C -> T	<i>srap-1</i>	Encodes a mucin (ECM proteins)	A/V
+3.46	11368853	C -> T	<i>clh-2</i>	Chloride channel protein required for embryonic viability	S/F
+3.79	11597109	C -> T	<i>npp-5</i>	Embryo development and reproduction	R/H

Table 3: Mapping Data

Chromosome	SNP site	N2	Het	S	Total	%N2	%Het	%S
I	-2.89	0	7	5	12	0%	58%	42%
	2	8	5	8	21	38%	24%	38%
	28.42	1	0	11	12	8%	0%	92%
II	-15.59	6	3	26	35	17%	9%	74%
	-8.26	6	5	18	29	21%	17%	62%
	-6.31	4	1	2	7	57%	14%	29%
	-4.74	1	0	6	7	14%	0%	86%
	-2.54	2	1	31	34	6%	3%	91%
	-1.07	2	0	0	2	100%	0%	0%
	-0.98	2	0	0	2	100%	0%	0%
	-0.46	1	1	0	2	50%	50%	0%
	-0.03	0	1	1	2	0%	50%	50%
	0	0	1	1	2	0%	50%	50%
	0.49	0	0	2	2	0%	0%	100%
	0.6	0	0	16	16	0%	0%	100%
	0.76	1	0	0	1	100%	0%	0%
	0.94	1	0	34	35	3%	0%	97%
	3.13	1	1	46	48	2%	2%	96%
	3.36	1	2	46	49	2%	4%	94%
	3.79	1	2	44	47	2%	4%	94%
	6.8	2	4	43	49	4%	8%	88%
	12	5	6	40	51	10%	12%	78%
	17.03	4	11	19	34	12%	32%	56%
22.96	4	12	20	36	11%	33%	56%	
V	-17.81	8	0	4	12	67%	0%	33%
	-11.7	6	0	5	11	55%	0%	45%

Table 4: Neuronal and Muscle Marker Transgenes and Strains Used

Strain Number	Allele	Genotype/Gene	Expression Pattern/ Phenotype
CZ333	<i>juls1</i>	<i>Punc-25-SNB::GFP</i>	GABAergic synapses
CZ1200	<i>juls76</i>	<i>Punc-25::GFP</i>	GABAergic neurons
KP2229	<i>nuls94</i>	<i>Pacr-2-GFP::SNB-1</i>	Cholinergic synapses
KP3292	<i>nuls152</i>	<i>Punc-129-SNB-1::GFP, ttx-3::RFP</i>	Cholinergic synapses
KP5864	<i>nuls321</i>	<i>Punc-15-mCherry</i>	Cholinergic neurons
RP1	<i>trls10</i>	<i>myo-3p::MB::YFP, myo-2p::YFP, ceh-23::HcRed, unc-25::DsRed, unc-129nsp::CFP</i>	Muscle membranes

Table 5: *pxn-2* with Neuronal and Muscle Marker Transgenes Generated and/or Imaged

Strain Number	Genotype	Phenotype
CZ29133 *	<i>juls1; ju358</i>	unsuppressed <i>pxn-2</i> with GABAergic synapses
CZ24632	<i>juls1; ju1123; tm3464</i>	suppressed <i>pxn-2</i> with GABAergic synapses
CZ25063	<i>juls76; ju1123; tm3464</i>	suppressed <i>pxn-2</i> with GABAergic neurons
CZ24520	<i>nuls94; ju358</i>	unsuppressed <i>pxn-2</i> with Cholinergic synapses
CZ24521	<i>nuls94; ju1123; tm3464</i>	suppressed <i>pxn-2</i> with Cholinergic synapses
CZ24795	<i>nuls152; ju1123; tm3464</i>	suppressed <i>pxn-2</i> with Cholinergic synapses
CZ25064	<i>nuls321; nuls152; ju1123; tm3464</i>	<i>suppressed pxn-2 with Cholinergic neurons and synapses</i>
CZ25351	<i>trls10; ju1123; tm3464</i>	suppressed <i>pxn-2</i> with muscles

*Generated by Jennifer Gotenstein

Table 6: Rescue Strains

Strain Number	Genotype	DNA in Transgene	Method	Phenotype
CZ26369	<i>pmyo-2:juEx7869</i>	Fosmid WRM0626cC02	Injected into N2 with <i>pmyo-2</i>	RFP+ in pharynx
CZ26370	<i>pmyo-2:juEx7870</i>	Fosmid WRM0626cC02	Injected into N2 with <i>pmyo-2</i>	RFP+ in pharynx
CZ26371	<i>pmyo-2:juEx7871</i>	Fosmid WRM0626cC02	Injected into N2 with <i>pmyo-2</i>	RFP+ in pharynx
CZ26372	<i>ju430:ju1185;</i> <i>juEx7869</i>	Fosmid WRM0626cC02	Crossed to <i>ju430:ju1185</i>	Increased suppression of lethality and RFP+ in pharynx
CZ26373	<i>ju430:ju1185;</i> <i>juEx7871</i>	Fosmid WRM0626cC02	Crossed to <i>ju430:ju1185</i>	Increased suppression of lethality and RFP+ in pharynx

Table 7: Additional Strains Generated for Analysis of *pxn-2* Mutants

Strain Number	Genotype
CZ23108	<i>ju1299; ju432</i>
CZ23109	<i>ju1299; ju358</i>
CZ23452	<i>ju1123; uncdpy/eps-8</i>
CZ23947	<i>mup-4/+; ju1123</i>
CZ23862	<i>ju1123; k193</i>
CZ24028	<i>ju1123; b246</i>
CZ24298	<i>ju1300; ju358</i>
CZ24951	<i>tm3464/+; ju1176</i>
CZ24983	<i>ok785; b246</i>
CZ25227	<i>ju1198; tm3464</i>
CZ26030	<i>ju1190</i>
CZ26149	<i>ju1190; tm3464/+</i>
CZ24794	<i>ju1176</i>

Table 8: Primer Sequences**A. Mapping Primers**

SNP Location	Digesting Enzyme	Forward Primer Sequence	Reverse Primer Sequence
I-2.89	HaeII	TGTTGCTTGTTGTGAACCTC	ACCACCGTATCTCTTTCCCTGC
I+2	BanII	GCAATGGTGTACGGTGAAAC	TTGGCAAGGGAGCATTCTTC
I+28.42	KpnI	AAAGCTATCTCCCGTTTCGC AC	TTCAGCAGAGATGGGTGTATCG
II-15.59	ApoI	TCTCTGTGCTTCATGGATCTT C	ACTCTCGAATCAATGCCCAGC
II-8.26	HpyCH4IV	CACCAATTTGCGTCAGCTTA C	GAATTGGGCAATATACTCCGTG
II-6.31	TaqI	CACCACCGGAATGTTCCCTG	GGAAATGACCCACCGGACTAT G
II-4.74	BstNI	TCGACGAGTCACAGTTGACC	TCCTTCCTATGCAATCCCTTAC AC
II-2.54	AvaI	AAATACTGGCTGGTGATCCT CATG	AAATGCCGTTGACAGTCCCTC
II-1.07	N/A	ACGGCTGGTTGTTTGTAGAT ACG	CTCGCAGCGAATACAGAAGCT C
II-0.98	HpaII	GAAGGAAAGACTAGCCCATT TCAG	AATTTAGCCGTGTACGAATCC
II-0.46	N/A	TCTCGTTGCGTCTCGTCTCG	AAACTGGCATTTCGGCGTTTCG
II-0.03	N/A	AAAGAGCAGGTGTCAGGTTT G	AAACTAACATGGCACCCATTCC
II+0	N/A	GTATCCGGCACGATCTCCTC	GATCAAACGACGAGGCTGCAC
II+0.49	N/A	GAAGACTTCCTGTTCAAGCC AC	AAGTTCATTTGCCGCTCGATC
II+0.6	Hpy188III	CACGTCTCTAAACCCGATCC	CCAAGAGAACAGAGCCAAGG
II+0.76	N/A	CTGATCTCCTCTGGCTTGGA C	GGGACAGTTAGGACGCAGTAG
II+0.94	StyI	ACTGACCATTCTGAGGCTGT GAC	GTCCCTCCTGAACGGCAATATA CTC
II+3.13	HpyCH4IV	ATTCCGACACCAGAACGGAC	ATTTGAAGGATACACCGGGCTC
II+3.36	DraIII	GGAAGACCACGCAAACCGA C	TCACTCATTTCGGTTCACGAC
II+3.79	HhaI	ATACATGGTAGTCTTGCGTC AG	AAGTACACACCGATCACTGATG
II+6.8	AvaII	CAATGAATGCCGCAGATAGG	TAGCATATCTCGGTTTCAGTGG
II+12	NcoI	TGCGGCAGCGGATAAAGTTG	ATAGTAGCCTCCCGATCCCTG

Table 8: Primer Sequences, Continued.

A. Mapping Primers, Continued.

SNP Location	Digesting Enzyme	Forward Primer Sequence	Reverse Primer Sequence
II+17.03	Hpy188I	AATTCTTCCAGACGCCATCT ACTC	ATAGGCACACGCGAATTGATTG
II+22.96	BstYI	GCTTCGGAAACGTAAGTTGG	TATTATTATGCGGGCGGCACTG
V-17.81	AluI	GCATTTGGCACGTTGTGCTC	CGAGAAACGACAAATCCTGAA G
V-11.7	AatII	AAAGTATGTCTGCCGGTTGG	CCAAAGCAAACACTATCGGTGAG

B. Other Primers

Primer Name	Sequence
AC4095	TCTCGGAAGACCACGCAAAC
AC4096	ACAACGTCATCAGAGGTCAG

Table 9: Morphology of *spn-1* Mutants and Rescued Strains.
 Only transgenic animals are displayed in rescue strains.

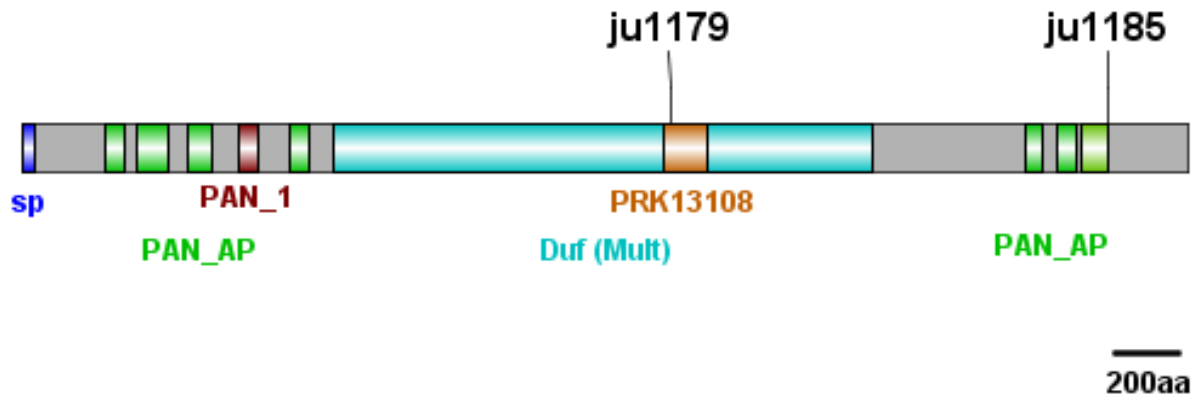
	Embryonic lethal	Larval lethal	Adult vab	Adult wild type	Total progeny analyzed
<i>ju430</i>	45.21%	16.09%	37.80%	0.89%	783
<i>ju430: ju1185</i>	84.65%	5.04%	2.88%	7.43%	417
<i>ju430: ju1185; juEx7869</i>	25.6%	4.7%	62.8%	7.0%	43
<i>ju430: ju1185; juEx7871</i>	13.4%	7.5%	61.2%	17.9%	67

Table 10: Brood Size of Vab Counts

	1	2	3	4	5	Average
<i>ju430</i>	130	139	234	-	218	180.25
<i>ju430: ju1185</i>	72	91	-	88	166	104.25
<i>ju430: ju1185; juEx7869</i>	99	95	80	128	49	90.2
<i>ju430: ju1185; juEx7871</i>	58	88	70	140	62	83.6

Figures

1a.



1b.

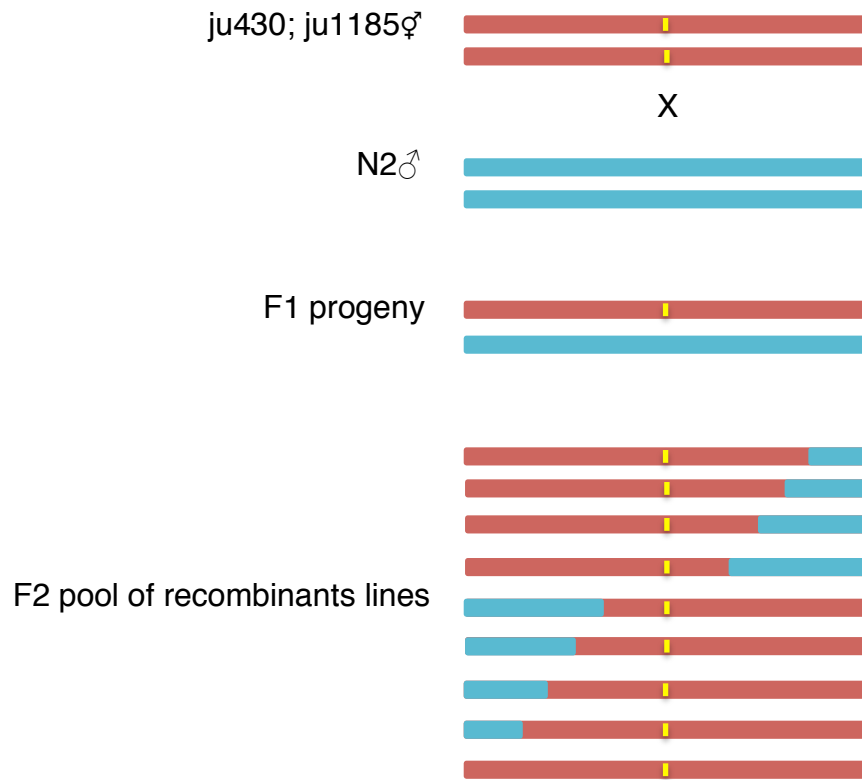
Allele	Codon change	Amino acid change	Residue #
ju1179	Aca->Gca	T->A	2041
ju1185	gCg->gTg	A->V	3426

Figure 1: Predicted Structure of *srap-1* and Location of Mutants.

1a: sp=signal sequence, PAN_AP=PAN Apple domain, PAN_1=PAN1 domain, Duf (mult) = multiple copies of an unknown domain adapted from Jones et al, 2012.

PRK13108 =prolipoprotein diacylglyceryl transferase from NCBI protein blast.

1b: *srap-1* alleles isolated from *ju430* EMS screen. The affected residue of *ju1179* is conserved in the PRK13108 domain. *ju1185* is not in a known domain.



Adapted from Doitsidou, 2010

Figure 2: Two point SNP Mapping Strategy to Generate Recombinant Lines

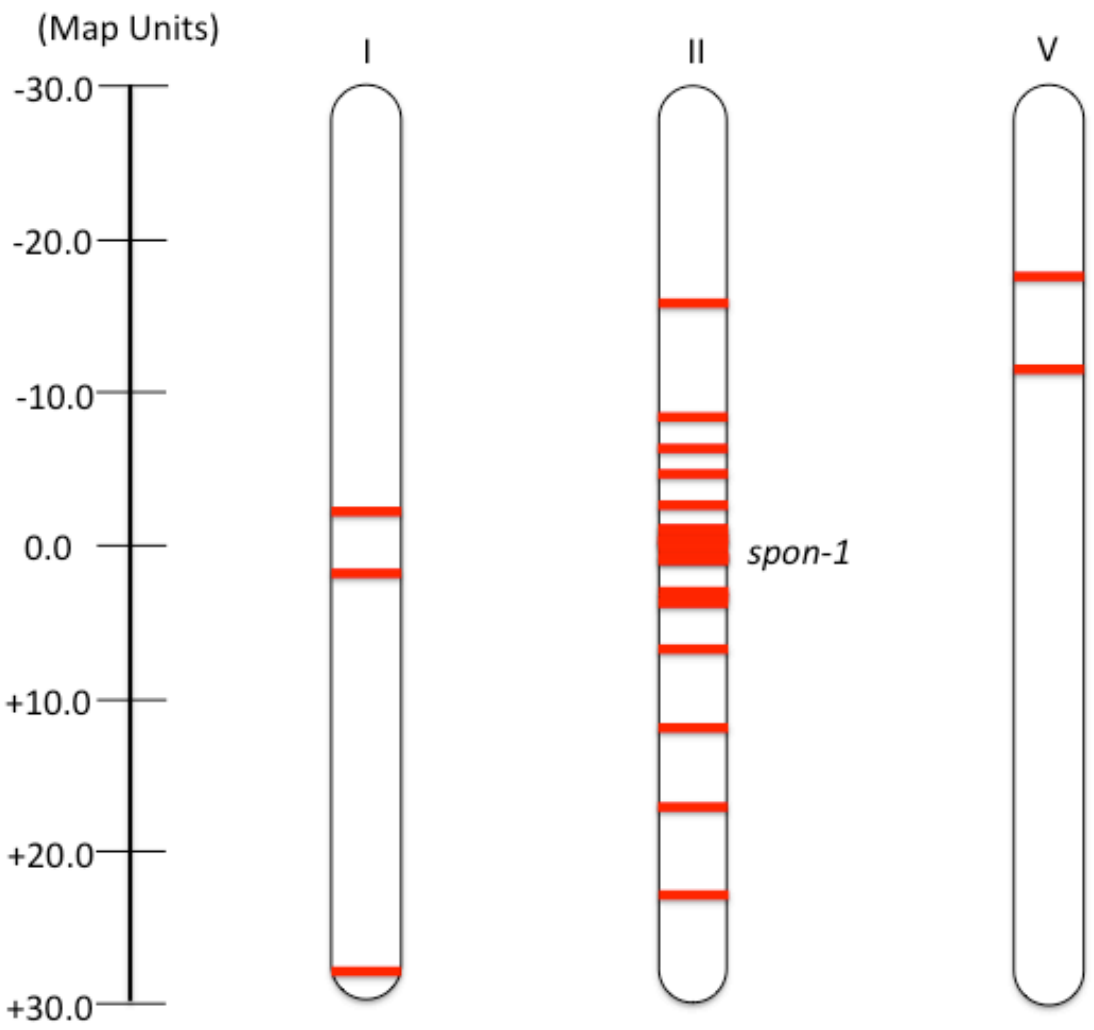


Figure 3: Tested SNP Sites on Chromosomes I, II, and V

Chromosome II												
Map Units	-2.54	-1.07	-0.98	-0.46	-0.03	0.0	+3.36	+3.79	+6.80	+12	+17.0	+22.9
31							S	S	S	N2	N2	N2
36							S	S	S	S	Het	Het
37							S	S	S	S	Het	S
38							S	S	S	S	Het	N2
39							S	S	S	S	Het	S
41							Het	Het	Het	Het	Het	Het
43	S						S	S	S	S	Het	Het
45	S						S	S	S	Het	Het	Het
46	S						S	S	Het	Het	Het	S
47	S						S	S	S	S	Het	N2
51	S						Het	Het	Het	Het	Het	Het
53	S						S	S	S	S	S	Het
54	S						S	S	S	S	S	Het
55	S						S	S	S	S	S	Het
56	S						S	S	S	S	N2	Het
57	S						S	S	Het	N2	N2	N2
72	S						S	S	S	N2		
75	Het						S	S	S	Het		
75	N2	N2	N2	N2	S	S	S	S	S	S		
.4												
77	S						S	S	S	Het		
80	N2	N2	N2	Het	Het	Het	S	S	S	S		
86	S						S	S	N2	N2		

Figure 4: Final SNP Summary Showing Recombination Occurring Through -0.46 on the Left and +6.80 on the Right

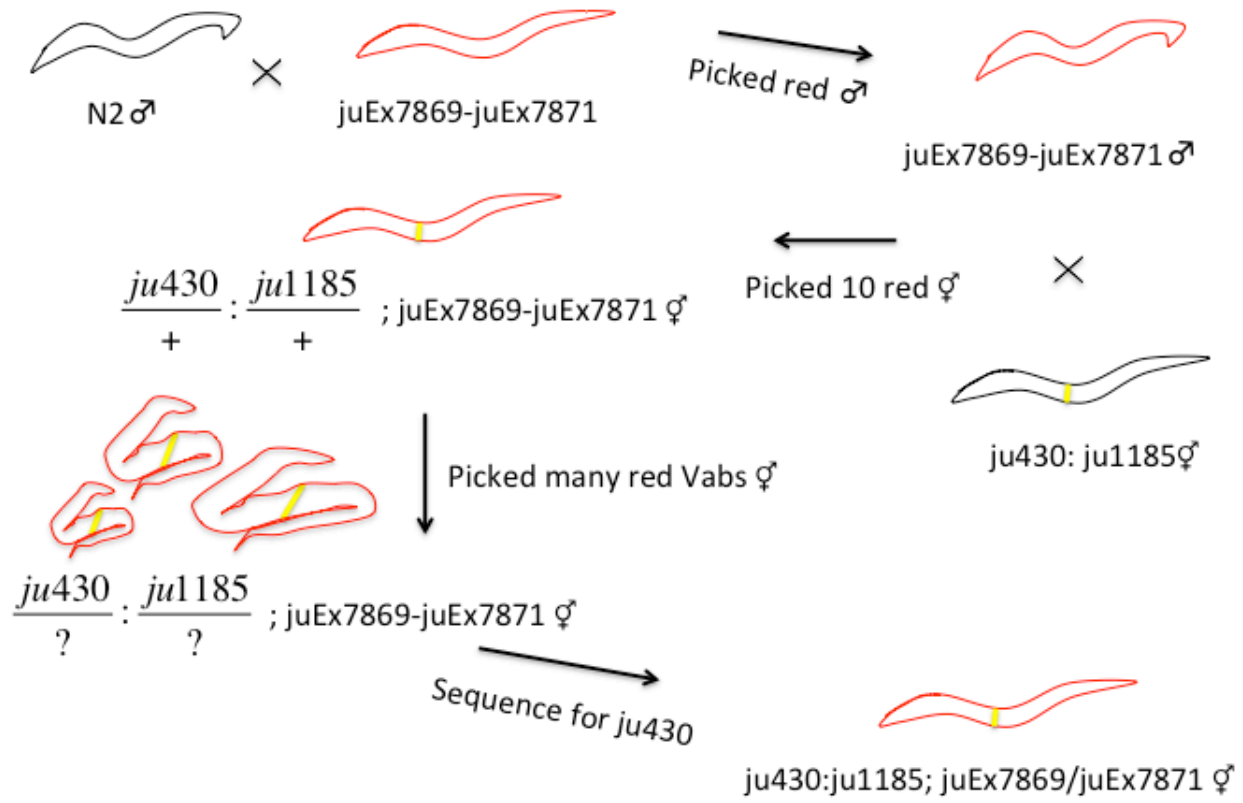


Figure 5: Genetic Cross of Transgenic Fosmid Animals with *ju430:ju1185*

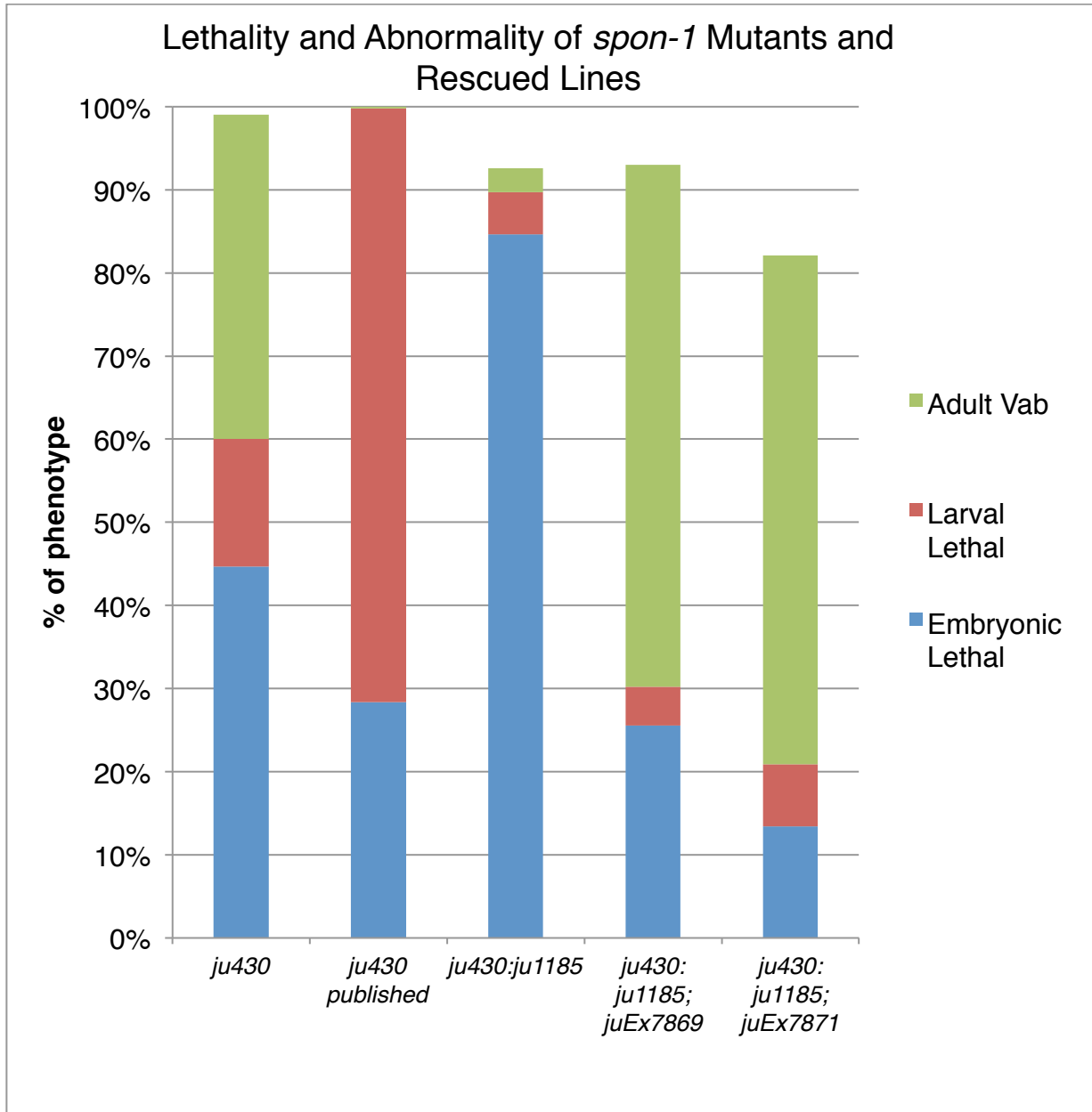


Figure 6: Lethality and Abnormality of Mutants and Rescued Lines

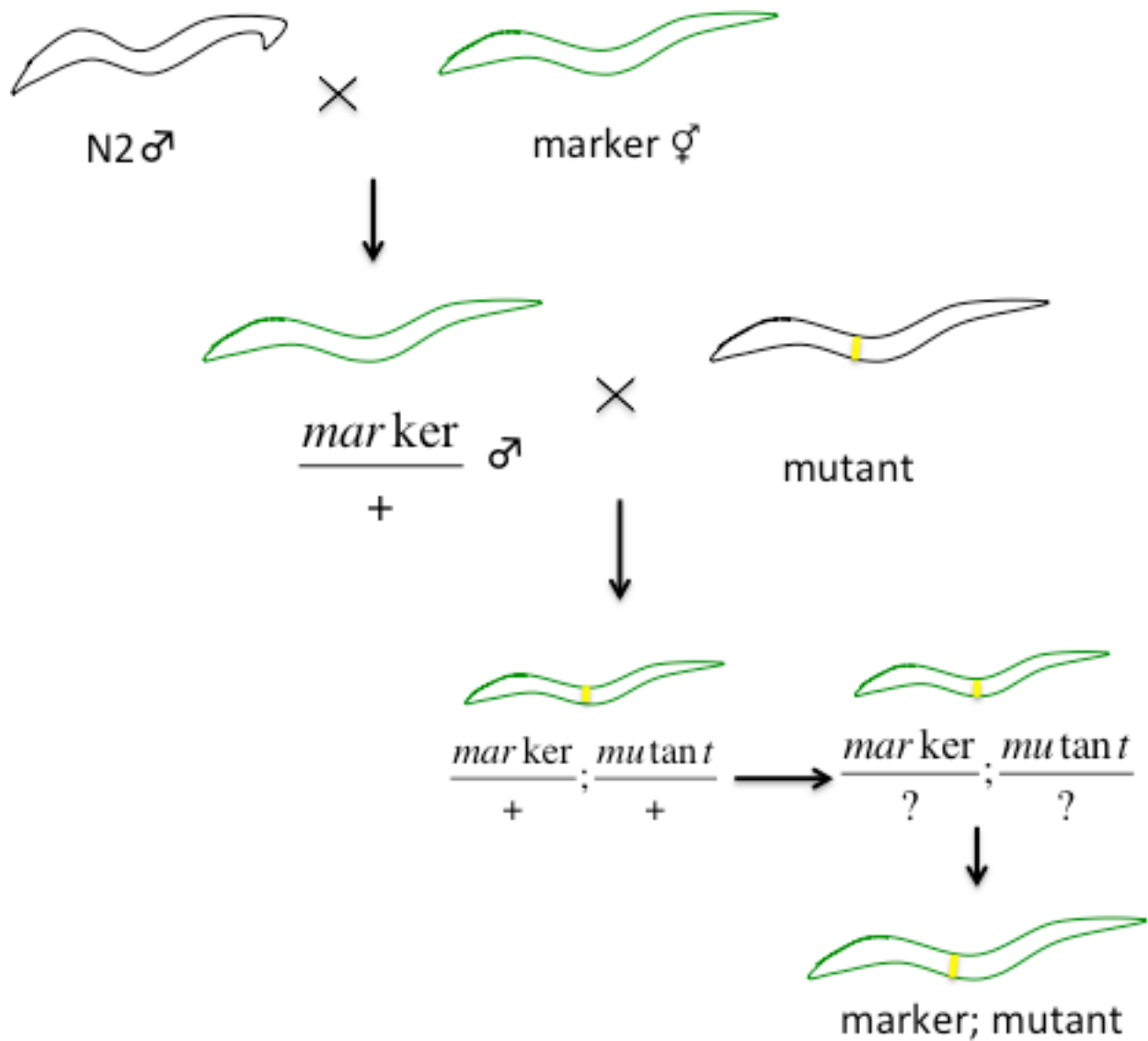


Figure 7: Genetic Crosses and Fluorescent Marker Strain Generation

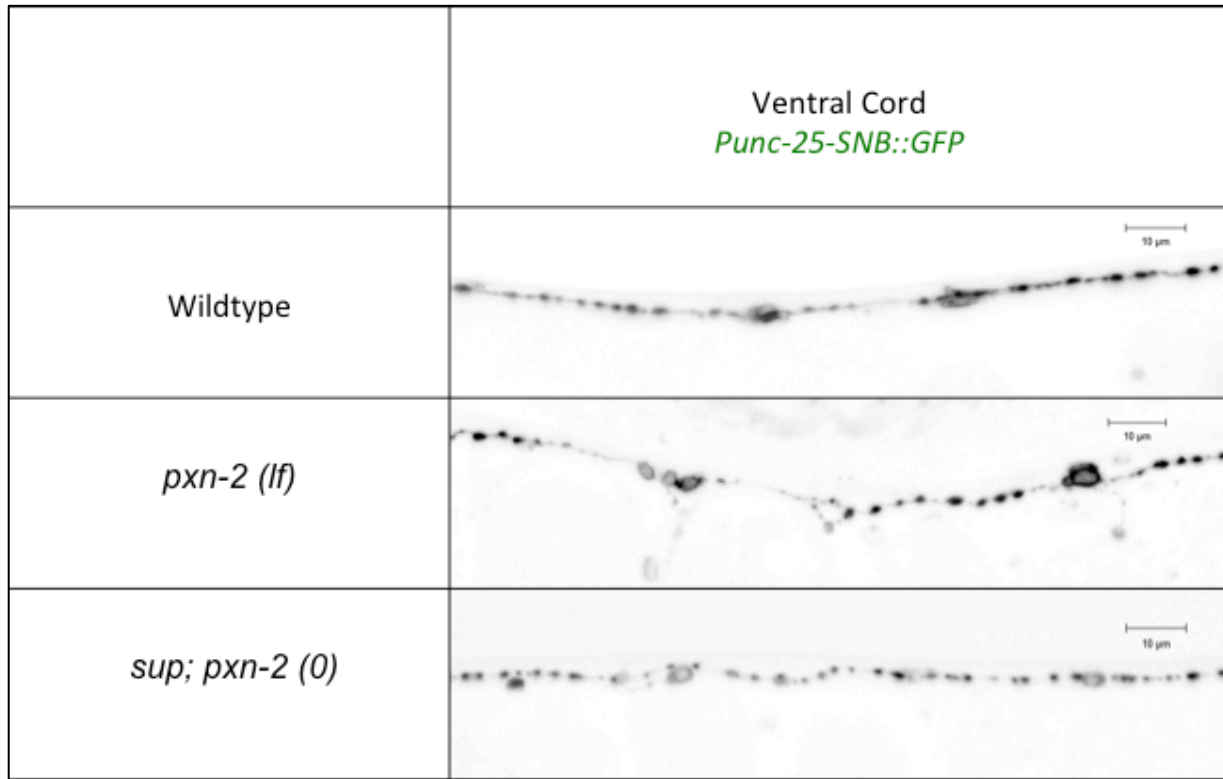


Figure 8: Imaging of Suppressed and Unsuppressed *pxn-2* using GABAergic Marker

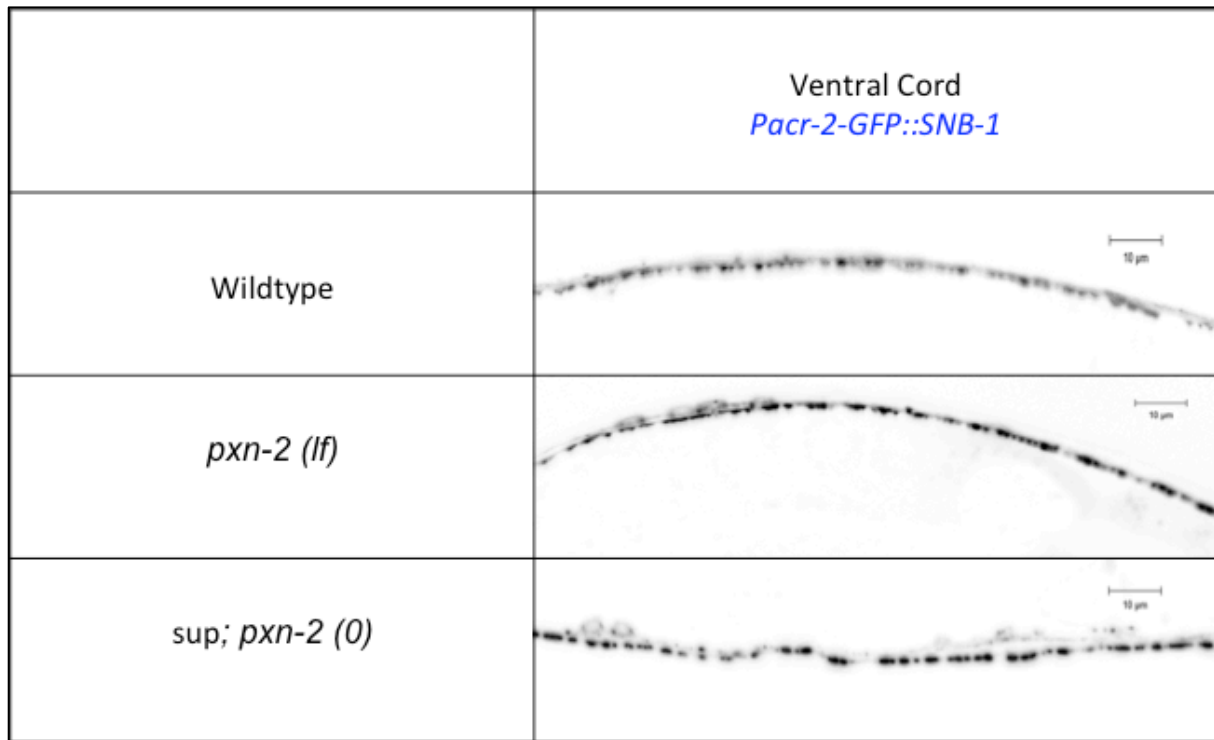


Figure 9: Imaging of Suppressed and Unsuppressed *pxn-2* using Cholinergic Marker

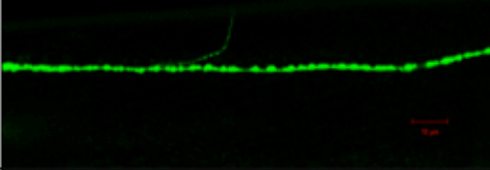
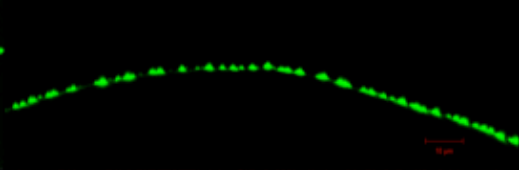
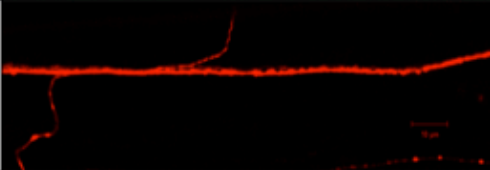
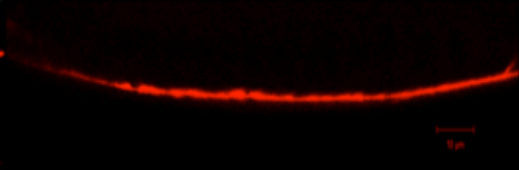
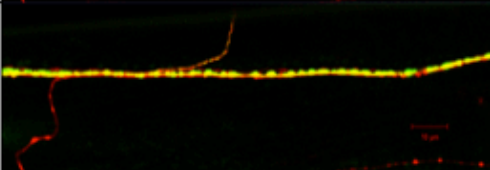
	<i>Punc-15-mCherry ; Punc-129-SNB-1::GFP, ttx-3::RFP;sup; pxn-2 (0)</i>	Wildtype
<i>Punc-129-SNB-1::GFP, ttx-3::RFP</i>		
<i>Punc-15-mCherry</i>		
Combined		

Figure 10: Imaging of Suppressed *pxn-2* using Synaptic & Whole Neuron Cholinergic Markers

References

- Chin-Sang, Ian D., and Andrew D. Chisholm. "Form of the worm: genetics of epidermal morphogenesis in *C. elegans*." *Trends in Genetics* 16.12 (2000): 544-51. Web.
- Chisholm, A.D. and Hardin, J. Epidermal morphogenesis (December 01, 2005), *WormBook*, ed. The *C. elegans* Research Community, WormBook, doi/10.1895/wormbook.1.35.1
- Chisholm, Andrew D., and Tiffany I. Hsiao. "The *C. Elegans* Epidermis as a Model Skin. I: Development, Patterning, and Growth." *Wiley interdisciplinary reviews. Developmental biology* 1.6 (2012): 861–878. *PMC*. Web. 24 Apr. 2017.
- Corsi A.K., Wightman B., and Chalfie M. A Transparent window into biology: A primer on *Caenorhabditis elegans* (June 18, 2015), *WormBook*, ed. The *C. elegans* Research Community, WormBook, doi/10.1895/wormbook.1.177.1, <http://www.wormbook.org>.
- Doitsidou, Maria, Richard J. Poole, Sumeet Sarin, Henry Bigelow, and Oliver Hobert. "C. elegans Mutant Identification with a One-Step Whole-Genome-Sequencing and SNP Mapping Strategy." *PLoS ONE*, vol. 5, no. 11, Aug. 2010, doi:10.1371/journal.pone.0015435.
- Fay, D. and Bender, A. SNPs: Introduction and two-point mapping (September 25, 2008), *WormBook*, ed. The *C. elegans* Research Community, WormBook, doi/10.1895/wormbook.1.93.2, <http://www.wormbook.org>.
- Ganz, Tomas. "Epithelia: Not Just Physical Barriers." *Proceedings of the National Academy of Sciences of the United States of America* 99.6 (2002): 3357–3358. *PMC*. Web. 29 Jan. 2017.
- Gotenstein, Jennifer R., Ryann E. Swale, Tetsuko Fukuda, Zilu Wu, Claudiu A. Giurumescu, Alexandr Goncharov, Yishi Jin, and Andrew D. Chisholm. "The *C. Elegans* Peroxidasin PXN-2 Is Essential for Embryonic Morphogenesis and Inhibits Adult Axon Regeneration." *Development* 137.21 (2010): 3603–3613. *PMC*. Web. 18 Jan. 2017.
- Halfter, Willi, Christophe Monnier, David Müller, Philipp Oertle, Guy Uechi, Manimalha Balasubramani, Farhad Safi, Roderick Lim, Marko Loparic, and Paul Bernhard Henrich. "The Bi-Functional Organization of Human Basement Membranes." *PLoS ONE* 8.7 (2013): n. pag. Web.

- Jones, Martin R., Ann M. Rose, and David L. Baillie. "Oligoarray Comparative Genomic Hybridization-Mediated Mapping of Suppressor Mutations Generated in a Deletion-Biased Mutagenesis Screen." *G3*, vol. 2, no. 6, 2012, pp. 657–663., doi:10.1534/g3.112.002238.
- Jones, Martin R., Ann M. Rose, and David L. Baillie. "The ortholog of the human proto-Oncogene ROS1 is required for epithelial development in *C. elegans*." *Genesis*, vol. 51, no. 8, 2013, pp. 545–561., doi:10.1002/dvg.22405.
- Kim, Hon-Song, and Kiyoji Nishiwaki. "Control of the basement membrane and cell migration by ADAMTS proteinases: Lessons from *C. elegans* genetics." *Matrix Biology* 44-46 (2015): 64-69. Web.
- Klar, Avihu, Mark Baldassare, and Thomas M. Jessell. "F-spondin: A gene expressed at high levels in the floor plate encodes a secreted protein that promotes neural cell adhesion and neurite extension." *Cell* 69.1 (1992): 95-110. Web.
- Kutscher L. M., Shaham S. Forward and reverse mutagenesis in *C. elegans* (January 17, 2014), *WormBook*, ed. The *C. elegans* Research Community, WormBook, doi/10.1895/wormbook.1.167.1, <http://www.wormbook.org>
- McCulloch, Katherine A., Yingchuan B. Qi, Seika Takayanagi-Kiya, Yishi Jin, and Salvatore J. Cherra III. "Novel Mutations in Synaptic Transmission Genes Suppress Neuronal Hyperexcitation in *Caenorhabditis Elegans*." *G3: Genes/Genomes/Genetics* 7.7 (2017): 2055–2063. *PMC*. Web. 29 Dec. 2017.
- Morrissey, M. A., and D. R. Sherwood. "An active role for basement membrane assembly and modification in tissue sculpting." *Journal of Cell Science* 128.9 (2015): 1661-668. Web.
- Rand, J.B. Acetylcholine (January 30, 2007), *WormBook*, ed. The *C. elegans* Research Community, WormBook, doi/10.1895/wormbook.1.131.1, <http://www.wormbook.org>.
- Woo, W.-M., E. C. Berry, M. L. Hudson, R. E. Swale, A. Goncharov, and A. D. Chisholm. "The *C. elegans* F-spondin family protein SPON-1 maintains cell adhesion in neural and non-neural tissues." *Development* 135.16 (2008): 2747-756. Web.
- Zhang. "Optimized CRISPR Design." *Optimized CRISPR Design*, 2017, crispr.mit.edu/.